



**Dynamical analysis
of sea-breeze
hodograph rotation in
Sardinia**

N. Moisseeva and
D. G. Steyn

This discussion paper is/has been under review for the journal Atmospheric Chemistry and Physics (ACP). Please refer to the corresponding final paper in ACP if available.

Dynamical analysis of sea-breeze hodograph rotation in Sardinia

N. Moisseeva and D. G. Steyn

The University of British Columbia, Department of Earth, Ocean and Atmospheric Sciences,
Vancouver, Canada

Received: 20 June 2014 – Accepted: 22 August 2014 – Published: 8 September 2014

Correspondence to: N. Moisseeva (nmoisseeva@eos.ubc.ca)

Published by Copernicus Publications on behalf of the European Geosciences Union.

Title Page

Abstract

Introduction

Conclusions

References

Tables

Figures



Back

Close

Full Screen / Esc

Printer-friendly Version

Interactive Discussion



Abstract

This study investigates the diurnal evolution of sea-breeze rotation over an island in the mid-latitudes. Earlier research on sea-breezes in Sardinia shows that the on-shore winds around various coasts of the island exhibit both the theoretically predicted clockwise rotation as well as seemingly anomalous anti-clockwise rotation. A non-hydrostatic fully compressible numerical model (WRF) is used to simulate wind fields on and around the island on previously-studied sea-breeze days and is shown to accurately capture the circulation on all coasts. Diurnal rotation of wind is examined and patterns of clockwise and anti-clockwise rotation are identified. A dynamical analysis is performed by extracting individual forcing terms from the horizontal momentum equations. Analysis of several regions around the island shows that the direction of rotation is a result of a complex interaction between near-surface and synoptic pressure gradient, Coriolis and advection forcings. An idealized simulation is performed over an artificial island with dramatically simplified topography, yet similar dimensions and latitude to Sardinia. Dynamical analysis of the idealized case reveals a rather different pattern of hodograph rotation to the real Sardinia, yet similar underlying dynamics. The research provides new insights into the dynamics underlying sea-breeze hodograph rotation, especially in coastal zones with complex topography and/or coastline.

1 Introduction

Sea-breeze (SB) circulation is a mesoscale phenomenon driven by a mesoscale, horizontal pressure gradient resulting from the differential heating of land and water. Recently, with the availability of fully compressible three-dimensional non-hydrostatic numerical models there has been a tremendous improvement in our understanding of the complex nature of SB and the associated non-linear interactions on several scales, from meso- β to micro-scale (Miller et al., 2003). Due to this complexity, numerical models present the only tool for studying the dynamics of SB circulation over real

Dynamical analysis of sea-breeze hodograph rotation in Sardinia

N. Moisseeva and
D. G. Steyn

Title Page

Abstract

Introduction

Conclusions

References

Tables

Figures



Back

Close

Full Screen / Esc

Printer-friendly Version

Interactive Discussion



domains with complex topography. As shown by Zhang (2005), Ramis and Romero (1995), Steyn and Kallos (1992), Mahrer and Segal (1985) and Walsh (1974) the general structure and diurnal cycle of the SB circulation can be well reproduced by a numerical model and agrees closely with the aspects developed by theoretical studies and observations.

Crosman and Horel (2010) conducted a thorough review of existing literature on numerical studies of SBs to summarize the current state of knowledge of the dependence of SB on geophysical variables. Despite the large numbers of scientific studies devoted to the subject, Crosman and Horel have identified several gaps in understanding of SB circulation. Among them is the ambiguity associated with SB dependence on topography and anti-clockwise hodograph rotation.

The mechanism behind the SB rotation was first explained by Haurwitz (1947), as an effect of the Coriolis force. One can therefore expect all SBs in the Northern Hemisphere and their corresponding hodographs to rotate clockwise. However, a number of cases have been identified where an apparently anomalous anti-clockwise hodograph rotation (ACR) was observed. Neumann (1977) showed, using a two-dimensional sea and land-breeze model, that the rate of turning of the direction of sea and land-breezes is far from uniform over the diurnal cycle. Simpson (1996) expanded on the analysis proposed by Neumann and concluded that in general the Coriolis force, which is the primary factor driving typical clockwise hodograph rotation (CR) in the Northern Hemisphere, is not always the most important term in the equations of motion. Kusuda and Alpert (1983) considered the issue analytically and described hodographs in terms of phase shifts. Using a linear model they showed that ACR hodograph rotation can be generated by including an ACR thermal force. The switch to ACR occurs at a critical value, which is a function of friction and latitude. They also employed a simple two-dimensional model with artificial topography and found that the dominant term inducing the rotation was a combination of pressure and surface gradient. In contrast to primarily analytical and idealized work, Steyn and Kallos (1992) used a three-dimensional numerical mesoscale model to study the issue in the Attic Peninsula, Greece. Their

**Dynamical analysis
of sea-breeze
hodograph rotation in
Sardinia**

N. Moisseeva and
D. G. Steyn

Title Page

Abstract

Introduction

Conclusions

References

Tables

Figures



Back

Close

Full Screen / Esc

Printer-friendly Version

Interactive Discussion



Dynamical analysis of sea-breeze hodograph rotation in Sardinia

N. Moisseeva and
D. G. Steyn

Title Page

Abstract

Introduction

Conclusions

References

Tables

Figures

◀

▶

◀

▶

Back

Close

Full Screen / Esc

Printer-friendly Version

Interactive Discussion



findings were in agreement with Kusuda and Alpert (1983) as well as local observations. The paper demonstrated that a balance of pressure and terrain gradient forcing is dominant, and can result in either CR or ACR. While the studies described present extremely valuable insight into the diurnal evolution of the SB, overall hodograph rotation has been largely neglected since the original study by Haurwitz (1947), according to Crosman and Horel (2010) who suggest simulating the hodograph rotation under a wide array of geophysical variables as a topic for future exploration.

Several studies have previously examined SBs in Sardinia (Dalu and Cima, 1983; Melas et al., 2000), which is located in the Western Mediterranean Sea and provides an ideal platform for investigation of SB dynamics in the mid-latitudes. SBs are known to be fairly frequent in the Mediterranean region and rich meteorological datasets are readily available from fifty meteorological stations on the island, of which twelve coastal locations are shown on Fig. 1. Sardinia has a complex topography with three mountain ranges situated slightly closer to the eastern side of the island. The island is approximately elliptical in shape, with length and width 270 km and 140 km, respectively.

A recent study by Furberg (2002) focused on developing a statistical climatology of SB in Sardinia based on data collected over approximately 16–26 months using the network of 12 coastal stations shown in Fig. 1. The paper examines diurnal hodograph rotation and also shows that under appropriate conditions SB can develop simultaneously on all coasts of Sardinia, which is in close agreement with the finding of Melas et al. (2000). More importantly, the study demonstrates using averaged wind hodographs that both CR and ACR are known to occur along the coast of the island. These findings provide an extremely useful starting point for numerical modeling of the SB circulation and hodograph rotation in Sardinia.

2 Methods

2.1 Model setup

The Weather Research and Forecast Model (WRF-ARW) is used to simulate seven SB episodes during warmer months of 1997–1998 in Sardinia identified in Furberg's (2000) work. While the model offers great operational forecasting capabilities, effectively no options for dynamical analysis are available, which presents a serious limitation to those using WRF for research: while the model demonstrates excellent performance and accuracy it does not allow one to investigate the dynamics driving the modelled phenomena. In order to overcome this limitation the model code was adjusted to allow for the extraction of the individual tendency terms of the horizontal momentum equations. The details of the introduced changes, as well as modified code are available as Supplement.

The knowledge that the episode days identified by Furberg (2000) had favorable atmospheric conditions for the formation of SB on the island provides an extremely useful starting point for the numerical simulation. Identified primarily on the basis of diurnal reversal of surface wind direction, first suggested by Steyn and Faulkner (1986) the following days were considered SB days on Sardinia:

- 17 May 1997
- 15 August 1997
- 20 May 1998
- 30 May 1998
- 20 June 1998
- 21 June 1998
- 29 June 1998

Identical domain configuration was used for all of the SB episode days. The simulation was set up on a two-way nested domain centered on the island of Sardinia with 50

Dynamical analysis of sea-breeze hodograph rotation in Sardinia

N. Moisseeva and
D. G. Steyn

Title Page

Abstract

Introduction

Conclusions

References

Tables

Figures



Back

Close

Full Screen / Esc

Printer-friendly Version

Interactive Discussion



squared error (RMSE) between model and observation, and hence corresponding to the primary direction of air flow.

Note that the modelled and observed onshore directions were defined separately for the observed and modelled winds and allowed to differ for each individual day.

While these directions were generally found to be in close agreement, several stations showed a considerable discrepancy between model and observations (e.g. Valledoria, Jerzu). Introduction of this flexibility is a particularly important aspect of the proposed evaluation methodology. While it may seem that this assumption makes the evaluation criteria less stringent, it in fact, acts as a filter to isolate the subgrid-scale effects that are inevitably present in observational data, and entirely absent from the model output. As the hourly winds are subsequently projected onto the identified onshore direction, a slight difference in the definition of the onshore axis due to inclusion/exclusion of the subgrid-scale effects can easily mask the model's overall good performance. The advantage of this approach is that it allows us to compare and evaluate the larger scale kinematics and their diurnal evolution, rather than the local effects due to subgrid-scale phenomena.

Overall, individual (non-averaged) daily hodographs present one of the most stringent criteria for model evaluation, as instantaneous wind data is inevitably highly variable. However, as seen in Fig. 2, there is good agreement between modelled and observed winds. While no observational record is present for Siniscola station for the modelled day, there appears to be a greater discrepancy between simulated and observed data on the eastern coast. Modelled winds at Jerzu station, located beneath the highest peak in Gennargentu Ranges (1834 m) (Fig. 1), are consistently inferior to simulations at other stations on all simulation days. This can likely be explained by steep topography in close proximity to the east coast, which presents a well known challenge for numerical models. The nonorthogonal grid lines introduced due to the use of terrain-following vertical coordinate in WRF are known to produce significant truncation errors when attempting to calculate horizontal gradients, leading to computational inaccuracy of advection, diffusion and pressure gradient terms (Yamazaki and Satomura, 2010).

**Dynamical analysis
of sea-breeze
hodograph rotation in
Sardinia**

N. Moisseeva and
D. G. Steyn

Title Page	
Abstract	Introduction
Conclusions	References
Tables	Figures
◀	▶
◀	▶
Back	Close
Full Screen / Esc	
Printer-friendly Version	
Interactive Discussion	



Dynamical analysis of sea-breeze hodograph rotation in Sardinia

N. Moisseeva and
D. G. Steyn

Title Page

Abstract

Introduction

Conclusions

References

Tables

Figures

◀

▶

◀

▶

Back

Close

Full Screen / Esc

Printer-friendly Version

Interactive Discussion



The simulated and observed wind fields were then projected onto the corresponding identified onshore direction for each station and compared. As seen in Fig. 3, the model evaluation demonstrates excellent agreement between model and observations, both due to exceptional model performance and successful evaluation strategy. Note that the stations where the onshore directions determined by RMSE differed considerably between model and observations still show strong agreement in the development and shape of the onshore wind component, suggesting that the overall structure of the SB at that location is well represented. WRF clearly captures the kinematics of the SB circulation, and hence can be used for further dynamical analysis of the SB structure.

3 Dynamical analysis of real-case simulation

3.1 Rotation of the horizontal wind

The horizontal momentum equations solved in WRF can be represented in simplified vector form as

$$\frac{\partial \mathbf{V}_h}{\partial t} = \frac{\partial \mathbf{V}_{pg}}{\partial t} + \frac{\partial \mathbf{V}_{adv}}{\partial t} + \frac{\partial \mathbf{V}_{cor}}{\partial t} + \frac{\partial \mathbf{V}_{hdif}}{\partial t} + \frac{\partial \mathbf{V}_{vdif}}{\partial t} \quad (1)$$

where \mathbf{V}_h is total horizontal velocity vector, $\mathbf{V} = (U, V)$ and subscripts pg, adv, cor, hdif, and vdif correspond to forcing due to pressure gradient, advection, Coriolis, horizontal and vertical diffusion. Taking the 850 mb pressure level to be representative of overlying synoptic weather conditions, the pressure gradient term \mathbf{V}_{pg} can be further separated into synoptic (syn) and surface (surf) forcing by assuming that

$$\mathbf{V}_{syn} = \mathbf{V}_{pg} (850 \text{ mb}) \quad (2)$$

The remaining pressure gradient forcing is then assumed to be due to surface effects, i.e.

$$\mathbf{V}_{surf} = \mathbf{V}_{pg} - \mathbf{V}_{syn} \quad (3)$$

It is important to note that the formulation of WRF-ARW does not allow us to further separate the pressure gradient forcing into components to isolate the effects of topography, coastline curvature and aspect, land/sea temperature contrast, roughness and other local features.

5 Full horizontal momentum equations considered for dynamical analysis then become

$$\frac{\partial \mathbf{V}_h}{\partial t} = \frac{\partial \mathbf{V}_{\text{surf}}}{\partial t} + \frac{\partial \mathbf{V}_{\text{syn}}}{\partial t} + \frac{\partial \mathbf{V}_{\text{adv}}}{\partial t} + \frac{\partial \mathbf{V}_{\text{cor}}}{\partial t} + \frac{\partial \mathbf{V}_{\text{hdif}}}{\partial t} + \frac{\partial \mathbf{V}_{\text{vdif}}}{\partial t} \quad (4)$$

Following Neumann (1977), the tendency of horizontal wind direction can be expressed as

$$10 \frac{\partial \alpha}{\partial t} = \frac{1}{V_h^2} \mathbf{k} \cdot \left(\mathbf{V}_h \times \frac{\partial \mathbf{V}_h}{\partial t} \right) \quad (5)$$

where α is the angle of local wind relative to the positive x-axis, \mathbf{V}_h is the horizontal wind vector, and \mathbf{k} is a vertical unit vector. Positive and negative values of $\frac{\partial \alpha}{\partial t}$ correspond to ACR and CR respectively. Expanding the cross product in Eq. (5) using the components of the total wind vector in Eq. (4) it is possible to compare the magnitudes of the terms contributing most strongly to the rotation.

3.2 Regional patterns of hodograph rotation

Using the definition of $\frac{\partial \alpha}{\partial t}$ in Eq. (5) it is possible to create contour maps of regions of CR and ACR for the simulated real domain. 20 June 1998 was selected as a test case, as it has shown strong agreement between model and observed hodographs based on the results of model evaluation. Hourly contours produce extremely complex patterns. As we are primarily interested in identifying possible invariant features of the circulation, daytime hourly $\frac{\partial \alpha}{\partial t}$ values were averaged between 09:00 to 17:00 UTC to produce $\frac{\partial \alpha_{\text{day}}}{\partial t}$. Figure 4 shows daytime regional patterns of CR ($\frac{\partial \alpha_{\text{day}}}{\partial t} < 0$) and ACR ($\frac{\partial \alpha_{\text{day}}}{\partial t} > 0$) for the real case simulation.

Dynamical analysis of sea-breeze hodograph rotation in Sardinia

N. Moisseeva and
D. G. Steyn

Title Page

Abstract

Introduction

Conclusions

References

Tables

Figures

◀

▶

◀

▶

Back

Close

Full Screen / Esc

Printer-friendly Version

Interactive Discussion



Dynamical analysis of sea-breeze hodograph rotation in Sardinia

N. Moisseeva and
D. G. Steyn

Title Page

Abstract

Introduction

Conclusions

References

Tables

Figures

◀

▶

◀

▶

Back

Close

Full Screen / Esc

Printer-friendly Version

Interactive Discussion

The southwestern region of the nested domain is dominated by strong CR. The CR pattern continues around the northern part of Sardinia. The SB circulation on the eastern coast of the island is largely ACR. The southern tip of Sardinia shows a switch between CR and ACR likely due to the presence of the southern mountain range – the Sulcis Mountains (Fig. 1). Overall the rotation pattern appears to respond to the local features of the terrain. The island of Corsica to the north of Sardinia exhibits a very complex pattern with several extremely sharp gradients in rate of change of direction. This can likely be explained by Corsica's much steeper topography and slopes and proximity to the boundary of the nested domain.

Also identified in Fig. 4 are four subregions off the southwestern, northwestern, southeastern and southwestern coasts of the island exhibiting either CR or ACR. Each subregion is a square of 8×8 grid points covering an area of 576 km^2 . These regions were selected for further dynamical analysis in an attempt to understand the underlying processes most strongly influencing the sense of wind rotation.

3.3 Relative importance of tendency terms

Expanding the cross product in Eq. (5) using the components of the total wind vector in Eq. (4) the total rate of rotation can be broken into individual forcing terms as follows:

$$\frac{\partial \alpha_{\text{tot}}}{\partial t} = \frac{\partial \alpha_{\text{surf}}}{\partial t} + \frac{\partial \alpha_{\text{syn}}}{\partial t} + \frac{\partial \alpha_{\text{cor}}}{\partial t} + \frac{\partial \alpha_{\text{adv}}}{\partial t} + \frac{\partial \alpha_{\text{hdif}}}{\partial t} + \frac{\partial \alpha_{\text{vdif}}}{\partial t} \quad (6)$$

where the subscripts correspond the various tendency components, consistent with terms in Eq. (4).

To apply the term-by-term analysis (Eq. 6) to each region identified in Fig. 4, the hourly tendency values for the selected grid points was extracted. They were subsequently normalized by the Coriolis parameter f to produce non-dimensional values, and also spatially averaged amongst the 64 grid-points for each hour. Figure 5 shows the diurnal evolution of the individual terms as well as their spatial standard deviation.

Dynamical analysis of sea-breeze hodograph rotation in Sardinia

N. Moisseeva and
D. G. Steyn

Title Page

Abstract

Introduction

Conclusions

References

Tables

Figures

◀

▶

◀

▶

Back

Close

Full Screen / Esc

Printer-friendly Version

Interactive Discussion

For Region 1 shown in Fig. 5 total clockwise rotation rate increases throughout the day reaching a peak around 15:00 UTC, as may be explained by the growth of the land–sea temperature contrast. As expected, the Coriolis component is one of the leading terms inducing CR, and remains constant. The surface gradient becomes increasingly important through the day, initially contributing slightly to ACR but subsequently turning strongly CR. Note that the surface gradient term includes the combined effects of surface slope, roughness, temperature and pressure gradient and hence is non-zero even though the sub-domain is located over water. The synoptic gradient acts largely in opposition to the surface gradients, likely due to the formation of SB return flow near 850 mb level. As expected this forcing is strongest around 1400. Advection effect is always clockwise, but is of secondary importance in this dynamical balance. Horizontal and vertical diffusion terms are largely insignificant in this and the remaining regions, as they were located off the coast where friction is of secondary importance. As SBs are mesoscale phenomena, their scale is not restricted to the immediate coastal region. Hence the analysis can be performed away from the regions of sharp gradients in topography, roughness, and temperature and still capture the dynamics of the phenomenon. Overall, the balance appears to be dominated by surface and synoptic pressure gradients and Coriolis.

While the Coriolis term remains one of the largest in magnitude acting clockwise for Region 2, the combined effects of surface and synoptic pressure gradients outweigh its influence and induce ACR. Similarly to Region 1, a relatively small clockwise advection term is present. While clockwise Coriolis forcing remains the largest term throughout the course of the day the combined anti-clockwise effects of all remaining terms induce ACR in Region 3. A particular feature of the dynamics of this region is that the advection term is relatively important, and without it the ACR would not be possible. Region 4 exhibits largely CR, dominated by the combined effect of Coriolis and pressure gradient terms. Advection and synoptic act to induce ACR, but remain secondary.

It can hence be concluded that the sense of rotation is predominantly a result of local balance of Coriolis, surface and synoptic pressure gradients and advection. While

Dynamical analysis of sea-breeze hodograph rotation in Sardinia

N. Moisseeva and
D. G. Steyn

Title Page

Abstract

Introduction

Conclusions

References

Tables

Figures

◀

▶

◀

▶

Back

Close

Full Screen / Esc

Printer-friendly Version

Interactive Discussion



Coriolis forcing remains constant throughout the day, the remaining tendencies each have a unique diurnal pattern. Surface pressure gradient rotation tendency appears to respond faster to the increase in the land–sea temperature contrast, generally peaking in magnitude around noon. The forcing due to the synoptic pressure gradient appears to peak later in the day, which may be explained by the formation of the SB return flow, generally forming with a slight delay in response to the surface SB gravity wave (Miller et al., 2003). The advection term is largest around 15:00 UTC and can act to induce both clockwise and anti-clockwise rotation.

Hence, the dynamical balance of terms contributing to SB rotation in Sardinia appears to be much more complicated than that proposed by Steyn and Kallos (1992) for the Attic Peninsula. The rotation tendencies due to pressure gradients were not typically found to be the largest magnitude terms. Moreover, depending on the specific region of the domain these terms could be acting in the same or opposite directions. This work has shown that, rather than being the result of a simple balance of the synoptic and surface pressure gradients, the sense of direction is determined by whether the combined effects of surface, synoptic and advection tendencies outweigh the Coriolis effect.

The spatial pattern has also proved to be much more complex than that found in Steyn and Kallos (1992). One can speculate that the rotation patterns found around Corsica, which while having a significantly steeper topography closely resembles the single-hill structure of the Attic Peninsula, show a similar “CR tongue” formation near the eastern coast as found by Steyn and Kallos. However, the accuracy of the simulation was not evaluated in that region, and the proximity to the boundaries of the nest domain do not allow us to draw such conclusions with certainty. The complexity of the spatial patterns of SB rotation in Sardinia may also be explained by the increased ability of newer numerical models to capture detail. An idealized simulation was hence set up to determine whether the complexity of hodograph rotation patterns in Sardinia is associated with the specific topographic features of the island or improved numerical modelling abilities.

4 Dynamics of idealized case

It is important to highlight that the idealized case referred to herein is not to be confused with ideal-case WRF simulations, which introduce severe simplification into the model's operation. For this study the full features of a real-case WRF simulation were retained (including all surface, boundary layer and physics routines, as well as real earth features such as curvature and Coriolis). The term *idealized* in this case is meant to indicate that the shape, coastline and topography of the island were generalized to such an extent that they no longer represent the particular characteristics of Sardinia, but rather of any elliptical island with a bell-shaped topography in the mid-latitudes.

Using the standard WRF Preprocessing System (WPS) software to create a domain, the idealized case study was set up with the same parameters and nesting options as the real simulation. The topography was then manually edited to create a perfectly elliptical island in the center of the domain with 40 grid point semi-major axis and 18 grid point semi-minor axis, which approximately matches the size of Sardinia. The remaining grid points of the nest and parent domains were masked as water. All other standard fields such as land use, soil moisture and type, temperature and pressure were also adjusted. The topography height was edited to create a bell-shaped mountain with 800 m peak in the center of the island using a 2-D Hanning window.

Meteorological data from 20 June 1998 was used to create initial fields with WPS. These were again manually altered to fit the modified domain. Combined domain (including both static and meteorological fields) and boundary files generated by WRF had to be further adjusted to remove any inconsistencies arising due to interpolation. The rest of the simulation was performed using settings identical to the real cases. Since WRF was not designed to introduce idealized topography into a real-case simulation, the results presented in this section cannot be considered conclusive. The complexity of the WRF model makes tracking potential inconsistencies of these modifications extremely difficult. While the hourly patterns of hodograph rotation of the idealized simulation showed distributions nearly as complex as the real-case simulation, the diurnal

Dynamical analysis of sea-breeze hodograph rotation in Sardinia

N. Moisseeva and
D. G. Steyn

Title Page

Abstract

Introduction

Conclusions

References

Tables

Figures

◀

▶

◀

▶

Back

Close

Full Screen / Esc

Printer-friendly Version

Interactive Discussion

average shown in Fig. 6 does exhibit a much simpler pattern than that of a real case. Interestingly, regions of CR and ACR are arranged on opposite coasts to that of the real Sardinia, and similarly to Corsica from the real simulation and the Attic Peninsula from Steyn and Kallos (1992).

Overall the structure appears to be vortex-like, centering around the peak of the mountain. One can speculate that the region of CR on the eastern coast of the island is the equivalent of the “CR tongue” feature of Attic Peninsula. Again, further model analysis would be necessary to confirm this finding.

The term-by-term dynamical analysis for the idealized simulation is also much less conclusive than that of the real simulation. The west-coast ACR region shows consistent but relatively weak total rotation forcing, as seen in Fig. 7. Early morning values appear to be unrealistically large. This may be an indication of a model response to the morning switch in the direction of surface heat flux, which in some cases produces a spike in model fields. As likely inconsistencies in the domain set-up due to modification of the standard preprocessing routine may reduce the numerical stability of the model, the increased values caused by a spike may persist for long periods of time. Overall the dynamics of the ACR region mimic those of Region 3 in the real case simulation, with all significant terms acting to counterbalance Coriolis forcing. Since idealized Region 1 remains away from the coast the diffusion terms are again insignificant. Unlike the real case simulation the afternoon surface, synoptic pressure gradients and advection are all of approximately the same magnitude.

The CR region on the eastern coast (Region 2) of the idealized island shows much stronger rotational tendency than that on the western coast. The signs of surface and synoptic pressure gradient vary throughout the day. Similarly to idealized Region 1, pressure gradient and advection terms have like magnitudes. As this region partially covers land grid points vertical diffusion term can no longer be ignored. Friction effects contribute to the total balance inducing both clockwise and anti-clockwise rotation depending on the time of the day. Similarly to the real case, the overall shape of the total diurnal rotation curve appears to be strongly influenced by that of the surface pressure

**Dynamical analysis
of sea-breeze
hodograph rotation in
Sardinia**

N. Moisseeva and
D. G. Steyn

Title Page

Abstract

Introduction

Conclusions

References

Tables

Figures



Back

Close

Full Screen / Esc

Printer-friendly Version

Interactive Discussion



Dynamical analysis of sea-breeze hodograph rotation in Sardinia

N. Moisseeva and
D. G. Steyn

Title Page

Abstract

Introduction

Conclusions

References

Tables

Figures

◀

▶

◀

▶

Back

Close

Full Screen / Esc

Printer-friendly Version

Interactive Discussion



Lastly, an idealized simulation was attempted using a similar domain configuration as that of a real case, but introducing a completely artificial simplified topography. Contour maps of regions of CR and ACR showed the formation of a vortex-like region of ACR around most of the island, with a single protruding “tongue” of CR region in the middle of the East coast. The dynamical analysis of regions of CR and ACR showed that the balance of forces resembled those of the real simulation, however, higher variability as well as unlikely individual term magnitudes suggest that the simulation requires further improvements to be considered conclusive.

Acknowledgements. The authors would like to thank Alessandro Delitalaand and Maria Furberg for their help with SAR data. Reanalysis fields were provided by National Centers for Environmental Prediction (NCEP) and Computational and Information Systems Laboratory (CISL). Special thanks to Peter Jackson, Jim Dudhia and Anthony Toigo for their remote assistance with WRF. This work was funded by Natural Sciences and Engineering Research Council of Canada (NSERC) and IACPES CREATE program.

References

- Crosman, E. and Horel, J.: Sea and lake breezes: a review of numerical studies, *Bound-Lay. Meteorol.*, 137, 1–29, 2010. 22883, 22884
- Dalu, G. and Cima, A.: Three-dimensional airflow over Sardinia, *Il Nuovo Cimento*, 6, 453–472, 1983. 22884
- Furberg, M.: Sea breezes on Sardinia, Master’s thesis, Uppsala University, Sweden, 2000. 22885, 22886
- Furberg, M., Steyn, D., and Baldi, M.: The climatology of sea breezes on Sardinia, *Int. J. Climatol.*, 22, 917–932, 2002. 22884, 22898
- Haurwitz, B.: Comments on the sea-breeze circulation, *J. Meteorol.*, 4, 1–8, 1947. 22883, 22884
- Kusuda, M. and Alpert, P.: Anti-clockwise rotation of the wind hodograph. Part I: Theoretical Study, *J. Atmos. Sci.*, 40, 487–499, 1983. 22883, 22884, 22895
- Mahrer, Y. and Segal, M.: On the effects of islands’ geometry and size on inducing sea breeze circulation, *Mon. Weather Rev.*, 113, 170–174, 1985. 22883

22896

Dynamical analysis of sea-breeze hodograph rotation in Sardinia

N. Moisseeva and
D. G. Steyn

Title Page

Abstract

Introduction

Conclusions

References

Tables

Figures

◀

▶

◀

▶

Back

Close

Full Screen / Esc

Printer-friendly Version

Interactive Discussion



- Melas, D., Lavagnini, A., and Sempreviva, A.: An investigation of the boundary layer dynamics of Sardinia island under sea-breeze conditions, *J. Appl. Meteorol.*, 39, 516–524, 2000. 22884
- Miller, S., Keim, B., Talbot, R., and Mao, H.: Sea breeze: structure, forecasting, and impacts, *Rev. Geophys.*, 41, 1011, doi:10.1029/2003RG000124, 2003. 22882, 22892
- 5 Neumann, J.: On the rotation rate of the direction of sea and land breezes, *J. Atmos. Sci.*, 34, 1913–1917, 1977. 22883, 22889
- Ramis, C. and Romero, R.: A first numerical simulation of the development and structure of the sea breeze on the Island of Mallorca, *Ann. Geophys.*, 13, 981–994, doi:10.1007/s00585-995-0981-3, 1995. 22883
- 10 Simpson, J.: Diurnal changes in sea-breeze direction, *J. Appl. Meteorol.*, 35, 1166–1169, 1996. 22883
- Steyn, D. and Faulkner, D.: The climatology of sea-breezes in the Lower Fraser Valley, *B. C., Climatological Bull.*, 20, 21–39, 1986. 22885
- Steyn, D. and Kallos, G.: A study of the dynamics of hodograph rotation in the sea breezes of Attica, Greece, *Bound-Lay. Meteorol.*, 58, 215–228, 1992. 22883, 22892, 22894
- 15 Steyn, D., Ainslie, B., Reuten, C., and Jackson, P.: A retrospective analysis of ozone formation in the Lower Fraser Valley, British Columbia, Canada. Part I: Dynamical model evaluation, *Atmos. Ocean*, 51, 153–169, 2013. 22886
- Walsh, J.: Sea breeze theory and applications, *J. Atmos. Sci.*, 31, 2012–2026, 1974. 22883
- 20 Yamazaki, H. and Satomura, T.: Nonhydrostatic atmospheric modeling using a combined cartesian grid, *Mon. Weather Rev.*, 138, 3932–3945, 2010. 22887
- Zhang, Y., Chen, Y., Schroeder, T., and Kodama, K.: Numerical simulations of sea-breeze circulations over northwest Hawaii, *Weather Forecast.*, 20, 827–846, 2005. 22883

Dynamical analysis of sea-breeze hodograph rotation in Sardinia

N. Moisseeva and
D. G. Steyn

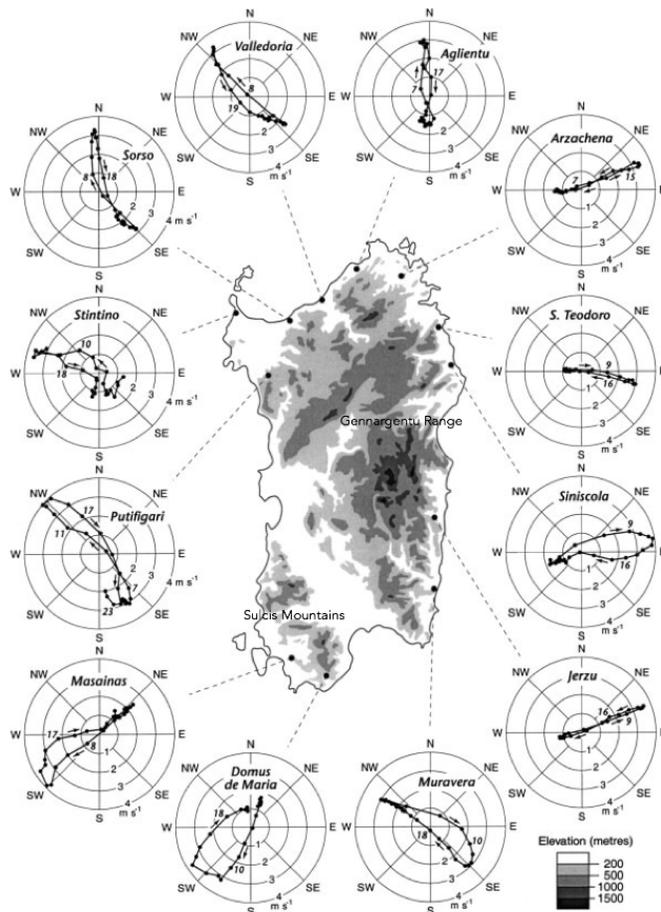


Figure 1. Topographic map of Sardinia with 12 coastal stations and SB hodographs. The island is approximately 270 km long and 140 km wide, from Furberg et al. (2002).

[Title Page](#)
[Abstract](#)
[Introduction](#)
[Conclusions](#)
[References](#)
[Tables](#)
[Figures](#)
[◀](#)
[▶](#)
[◀](#)
[▶](#)
[Back](#)
[Close](#)
[Full Screen / Esc](#)
[Printer-friendly Version](#)
[Interactive Discussion](#)

Dynamical analysis of sea-breeze hodograph rotation in Sardinia

N. Moisseeva and
D. G. Steyn

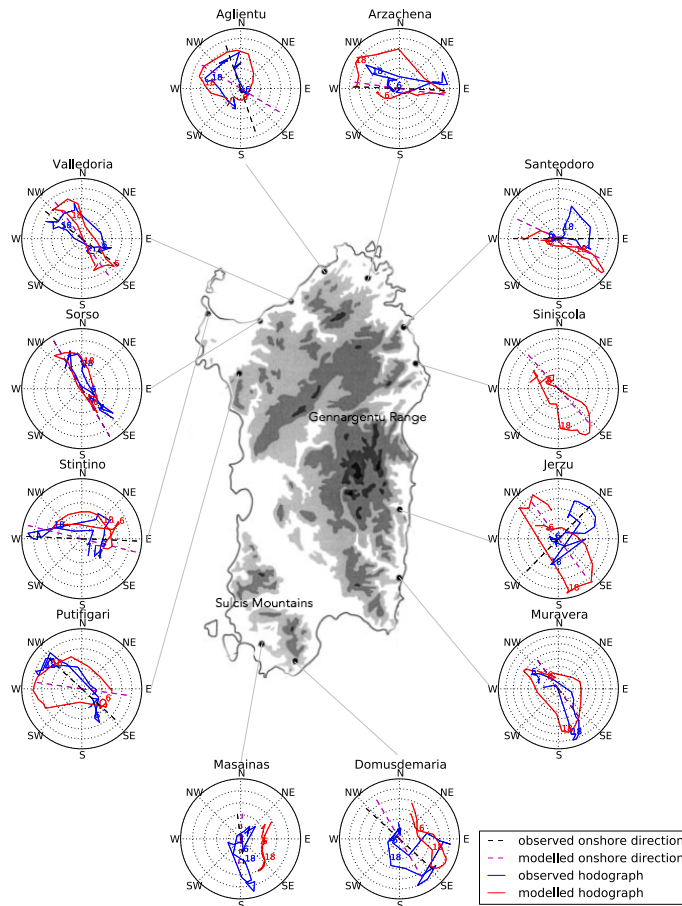


Figure 2. Modelled and observed wind hodographs at 10 m over Sardinia on 21 June 1998.

[Title Page](#)
[Abstract](#)
[Introduction](#)
[Conclusions](#)
[References](#)
[Tables](#)
[Figures](#)
[◀](#)
[▶](#)
[◀](#)
[▶](#)
[Back](#)
[Close](#)
[Full Screen / Esc](#)
[Printer-friendly Version](#)
[Interactive Discussion](#)

Dynamical analysis of sea-breeze hodograph rotation in Sardinia

N. Moisseeva and
D. G. Steyn

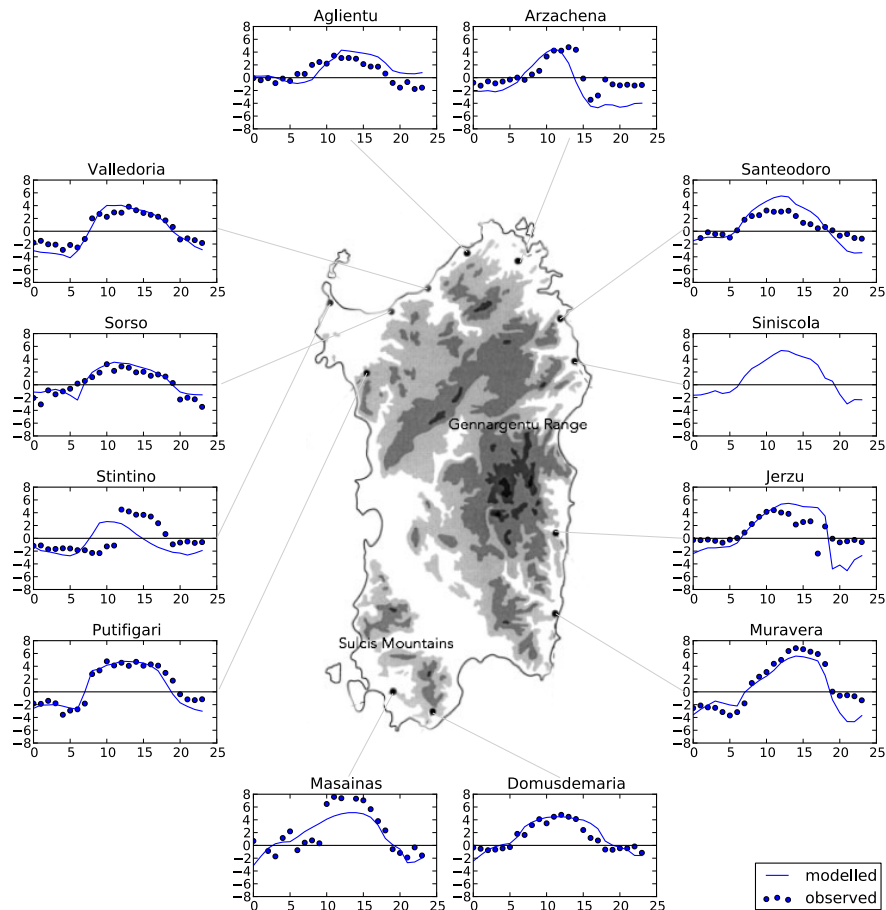


Figure 3. Diurnal evolution of onshore wind at 10 m over Sardinia on 21 June 1998.

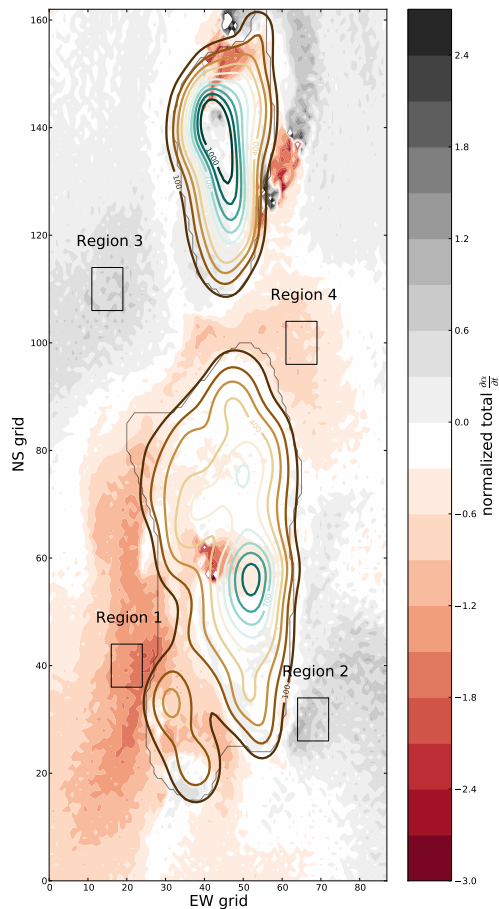


Figure 4. Total $\frac{\partial \alpha}{\partial t}$, averaged over daytime hours. Also shown: smoothed elevation contours, smoothed coast line, Regions 1, 2, 3, and 4 are identified for further dynamical analysis.

**Dynamical analysis
of sea-breeze
hodograph rotation in
Sardinia**

N. Moisseeva and
D. G. Steyn

Title Page

Abstract Introduction

Conclusions References

Tables Figures

◀ ▶

◀ ▶

Back Close

Full Screen / Esc

Printer-friendly Version

Interactive Discussion



**Dynamical analysis
of sea-breeze
hodograph rotation in
Sardinia**

N. Moisseeva and
D. G. Steyn

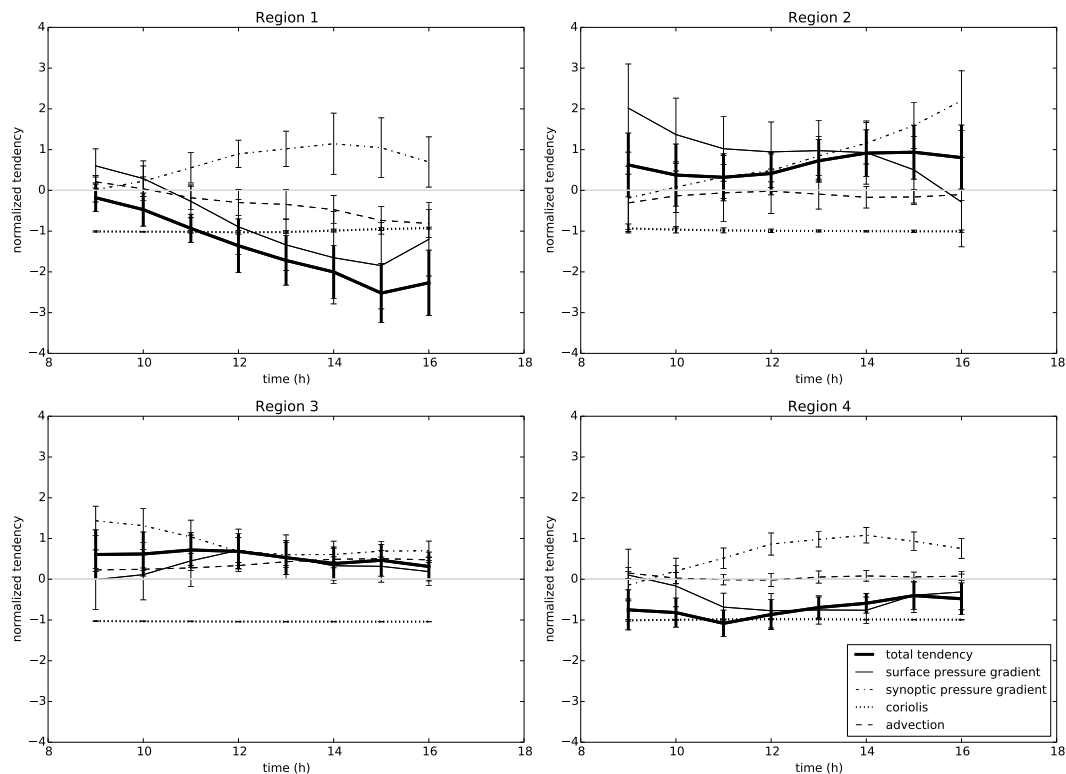


Figure 5. Evolution of dominant dynamic forcings for Regions 1, 2, 3, and 4, on 20 June 1998. Positive and negative values correspond to ACR and CR, respectively.

Title Page

Abstract

Introduction

Conclusions

References

Tables

Figures



Back

Close

Full Screen / Esc

Printer-friendly Version

Interactive Discussion



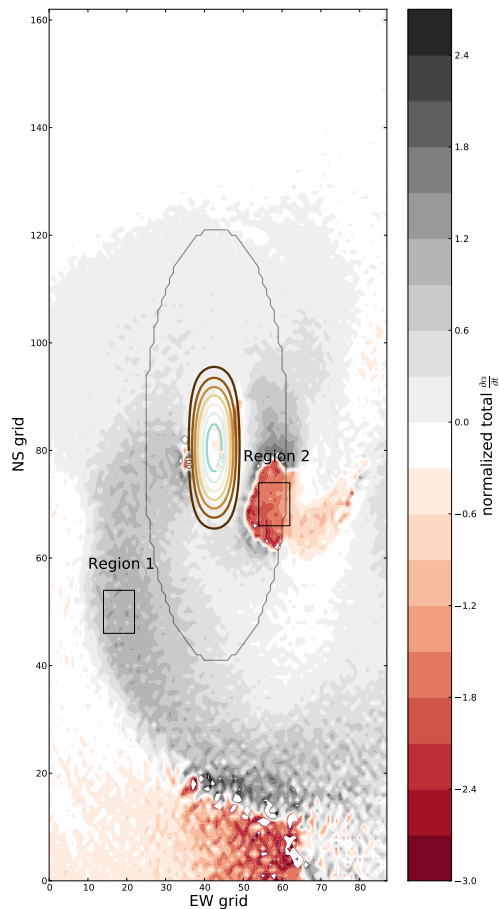


Figure 6. Total $\frac{\partial \alpha}{\partial t}$ values are averaged over daytime hours. Also shown: elevation contours, coastline, Regions 1 and 2 are identified for further dynamical analysis.

Dynamical analysis of sea-breeze hodograph rotation in Sardinia

N. Moisseeva and
D. G. Steyn

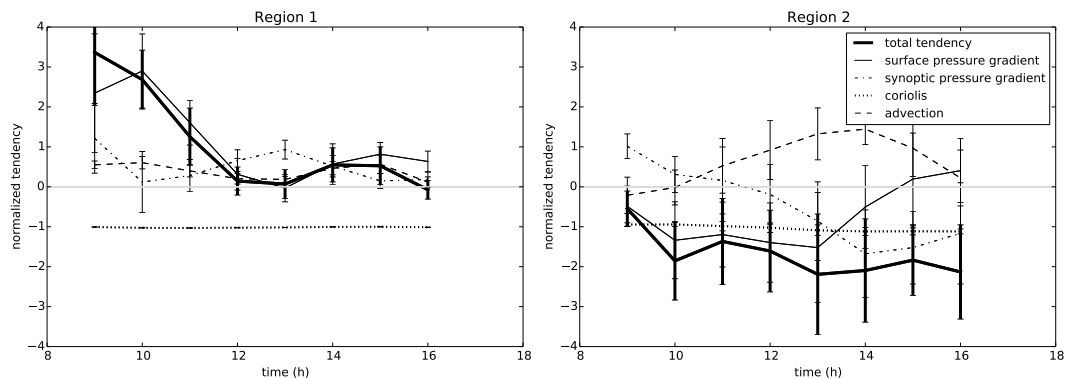


Figure 7. Evolution of dominant dynamic forcings for Regions 1 and 2, idealized case. Positive and negative values correspond to ACR and CR, respectively.

[Title Page](#)
[Abstract](#)
[Introduction](#)
[Conclusions](#)
[References](#)
[Tables](#)
[Figures](#)
[◀](#)
[▶](#)
[◀](#)
[▶](#)
[Back](#)
[Close](#)
[Full Screen / Esc](#)
[Printer-friendly Version](#)
[Interactive Discussion](#)